Desalination and Water Treatment
www.deswater.com
doi: 10.1080/19443994.2015.1041164

57 (2016) 10409–10421
May

Taylor & Francis
Taylor & Francis Group

Removal of secbumeton herbicide from water on composite nanoadsorbent

Imran Ali[a,*], Zeid A. Al-Othman[b], Abdulrahman Al-Warthan[b]

[a]*Department of Chemistry, Jamia Millia Islamia (Central University), New Delhi 110025, India, emails: drimran_ali@yahoo.com, drimran.chiral@gmail.com*
[b]*Department of Chemistry, College of Science, King Saud University, Riyadh 11451, Kingdom of Saudi Arabia, emails: zaothman@KSU.EDU.SA (Z.A. Al-Othman), awarthan@ksu.edu.sa (A. Al-Warthan)*

Received 30 January 2015; Accepted 24 March 2015

ABSTRACT

Water contamination by organic pollutants is a major problem. Secbumeton herbicide is a toxic pollutant and contaminates our water resources. Composite nanoadsorbent was prepared, characterized, and used for the removal of secbumeton from water by adsorption process. Secbumeton in water was analyzed by GC–MS under validated conditions. The optimized adsorption parameters were 30.0 μg/L concentration, contact time 30.0 min, pH 7.0, dose 2.5 g/L, and temperature 20.0°C, with 90% as removal capacity. The adsorbent was selective with respect to secbumeton. The results followed Langmuir, Freundlich, and Temkin models. The values of thermodynamic parameter i.e. ΔG° were −5.89, −5.81, and −5.71 kJ/mol at 20, 25, and 30°C temperatures. The value of ΔH° was −11.08 kJ/mol, indicating exothermic nature of adsorption. ΔS° value was -1.78×10^{-2} kJ/mol K; an indication of entropy decrease during adsorption. Kinetic modeling showed pseudo-second-order and liquid film diffusion mechanisms. The developed adsorption method was fast, eco-friendly, and economic as may be used at pHs of natural water bodies with low contact time and dose. This method may be used for the removal of secbumeton from any water body at large scale economically.

Keywords: Adsorption of secbumeton; Adsorption isotherms; Water treatment; GC–MS; Composite nanoadsorbent; Mechanisms of adsorption

1. Introduction

Secbumeton (*N*-ethyl-6-methoxy-*N*′-(1-methylpropyl)-*s*-triazine) is an important herbicide widely used for weed control due to its broad range of selective and non-selective applications [1–3]. It is useful for industrial weed control for a small time at specific place. But this herbicide is organic pollutant contaminating our environment; especially water resources [4–7]. The other toxicities of secbumeton include drowsiness, dizziness, gastric, and intestinal problems, skin dryness or cracking, corneal clouding, etc. Besides, it is also toxic to ecosystem and aquatic organisms such as fish algae, bacterial, etc. leading to disturbance to ecology and climate changes [4,8]. Secbumeton has been reported in various water bodies [9–11]. In view of these facts, it is very important to remove secbumeton from water.

A thorough search of literature indicates no method for the removal of secbumeton from water. Many methods may be applied for its removal, but adsorption is considered as the best one due to its

*Corresponding author.

wide range of applications, inexpensiveness, ease of operation, and universal nature [12–20]. Various types of adsorbents are available for the removal of different pollutants from water, but nanoadsorbents are gaining impetus in the present scenario. It is due to their unique features of adsorbing different pollutants from water [16]. Besides, composite nanomaterials can be moduled according to the requirement. Therefore, in this study iron nanoadsorbents were prepared by green technology [21]. Furthermore, iron nanomaterial was treated with 1-butyl-3-methylimidazolidium bromide to achieve composite nanomaterials for the efficient removal of secbumeton from water. The present article describes the removal of secbumeton from water. The residual secbumeton was monitored by GC–MS. The results of this study are present herein.

2. Experimental

2.1. Chemicals, reagents, and instruments

Secbumeton was obtained from Riedel-de-Haen (Seelze, Germany). 1-Butyl-3-methylimidazolidium bromide was obtained from Sigma-Aldrich Co., USA. Acetonitrile, acetone and methanol of HPLC grade were purchased from Merck India. Deionized water was prepared using Millipore-Q, Bedford, MA, USA system. GC–MS analyses were carried out using an Agilent Technology GC–MS system (Palo Alto, CA, USA) consisting of MS detector (model 5973), HP Ultra 2 capillary column (25 m × 0.2 mm i.d., and 0.33 μm film thicknesses), MSD ChemStation integrator and helium as a carrier gas. pH meter of Control Dynamics (Model APX175 E/C) was used to measure pH of the solutions. The centrifuge of Remi (model C-30BL) was used to separate the adsorbent. Powdered X-ray diffraction (XRD) was carried out on Philips PX-1830 diffractometer using Cu Kα radiation (λ = 1.54 Å), a Cu filter on secondary optics, 25 kV voltage, 30 mA current, and a proportional counter detector.

2.2. Preparation of composite nanoadsorbent

Iron nanoparticles (NPs) were prepared by green technology as per the standard procedure [22,23]. The black tea with 100.0 g/L concentrations was heated at 80˚C for 1 h. The extract was filtered and 0.20 M ferrous sulfate solution was added to tea extract in 1:2 ratios. This solution was kept for 24 h and the formed iron NPs were separated. NPs were washed with deionized water three times and dried in an over at 250˚C for 24 h. Five hundred milligram of 1-butyl-3-methylimidazolidium bromide was dissolved in 100 mL acetate buffer (0.05 M, pH 4.5). Five gram of NPs were transferred to 100 mL solution of 1-butyl-3-methylimidazolidium bromide. It was sonicated for 24 h. The treated iron NPs were separated and washed with deionized water three times and dried in an oven at about 100˚C for 24 h. The prepared composite NPs were ready for use in adsorption experiments as composite nanoadsorbent.

2.3. Characterization of composite nanoadsorbent

The prepared composite iron NPs were characterized by using UV–Vis spectrometry, SEM, and XRD techniques. The morphology of the material was characterized by field emission scanning electron microscope (FESEM). Images of samples were recorded at different magnifications at 10 kV operation. XRD patterns of native and composite iron NPs were obtained using Philips PX-1830 diffractometer using Cu Kα radiation (λ = 1.54 Å), a Cu filter on secondary optics, 25 kV voltage, and 30 mA current and a proportional counter detector. The NPs were scanned from 10˚ to 80˚ 2θ at a scanning rate of 3˚ 2θ per minute.

2.4. Preparation of secbumeton solutions

The standard solution of secbumeton (100 μg/mL) was prepared in methanol and stored in a freezer at −18˚C. The intermediate standards for GC–MS (0.50–80.0 μg/L) and adsorption studies (10–50 μg/mL) of secbumeton were prepared in methanol and water, respectively.

2.5. Adsorption studies

All the adsorption experiments were carried out on thermostatic water bath shaker at a fixed temperature for a given period of time. After adsorption, the solid and liquid parts were separated by centrifugation. Secbumeton concentrations in the solution samples were determined by GC–MS. Secbumeton adsorption isotherms were studied in the range of 10–50 μg/L as concentration with 1.0–10.0 pH range, 5–50 min contact time, 0.5–5.0 g/L dose, and 20.0–30.0˚C temperature. The various models were used to calculate isothermal and kinetic parameters. The data obtained in batch studies were used to calculate the equilibrium secbumeton uptake capacity. It was calculated using the following expression.

$$Q_e = (C_0 - C_e)/m \quad (1)$$

where Q_e is the amount (μg/g) of secbumeton adsorbed on adsorbent at equilibrium. C_0 is the initial concentration (μg/L). C_e is the equilibrium concentration (μg/L) at time "t". m is the weight of adsorbent in g/L. The percentage removal of secbumeton was calculated using the following equation.

$$\%\text{Removal} = [(C_0 - C_e)/C_0]100 \quad (2)$$

where C_0 and C_e have the usual meanings.

2.6. Kinetics studies

Kinetics for secbumeton adsorption was analyzed by ascertain uptake of secbumeton from aqueous solutions at different times. For studying adsorption isotherms, the different solutions of secbumeton were stirred with known amount of adsorbent till equilibrium. The residual secbumeton concentration was determined by GC–MS. The batch tests were carried out to compare the adsorptive capacities at different time intervals. A series of Erlenmeyer flasks (100 mL) having a definite volume of secbumeton solution of known concentrations were kept on a thermostatic water bath shaker. The known amount of composite nanoadsorbent was added to each flask with shaking. The solutions were centrifuged and the supernatants were analyzed for secbumeton. The blank runs with composite nanoadsorbent in 50.0 mL Millipore water were carried out under identical experimental conditions for the experimental errors.

2.7. GC–MS analysis

All qualitative and quantitative analyses of secbumeton were done by GC–MS system as described above. An aliquot of 2.0 μL containing secbumeton (100.0 μg/mL) was injected into the system. Helium gas was used as a carrier gas with a flow rate of 1.0 mL/min. All the experiments were carried out at 150°C and by an increase of 5°C/min up to 200°C temperature. Temperature of both GC oven and injector was 250°C. All the injections were made in split mode.

3. Results and discussion

3.1. Characterization of composite nanoadsorbent

The formation of iron NPs was confirmed by observing changing in peaks of tea polyphenols (205 nm) and caffeine (275 nm). It was observed that the intensities of these peaks deceased by addition of ferrous sulfate solution. This observation confirmed the formation of iron NPs. The FESEM images of iron NPs indicated spherical shape with diameter ranging 40–50 nm (Fig. 1). It is considered worthwhile that the polyphenols/caffeine present in tea extract were responsible in the formation of iron NPs due to reducing and capping behaviors of polyphenols/caffeine [22,23]. In XRD spectra, the peaks appeared at 25 and 29° θ related to FeOOH [iron(III) oxide-hydroxide] and Fe_2O_3 (maghemite) (Fig. 2). It is interesting to note that these peaks disappeared after treating iron NPs with 1-butyl-3-methylimidazolidium bromide. It was due to the fact that 1-butyl-3-methylimidazolidium bromide molecule reacted with iron NPs completely. This observation confirmed the formation of composite iron nanomaterial.

3.2. GC–MS analysis

Secbumeton was base lined separated with 8.50 min as the retention time. This herbicide was identified by running its standards under identical experimental conditions. The optimization of the separation was achieved by varying gas flow rate, temperature of injector, and column oven. Besides, MS detector optimization was also carried out to achieve the best separation. The amount (2.0 μL of 100.0 μg/mL) of herbicides loaded on GC instrument was also optimized. The flow rates of carrier gas were varied from 0.5 to 2.0 mL/min. Besides, the temperatures of injector and column were optimized using 150–300°C range. As a result of exhaustive experimentation, the best chromatographic conditions were developed and used.

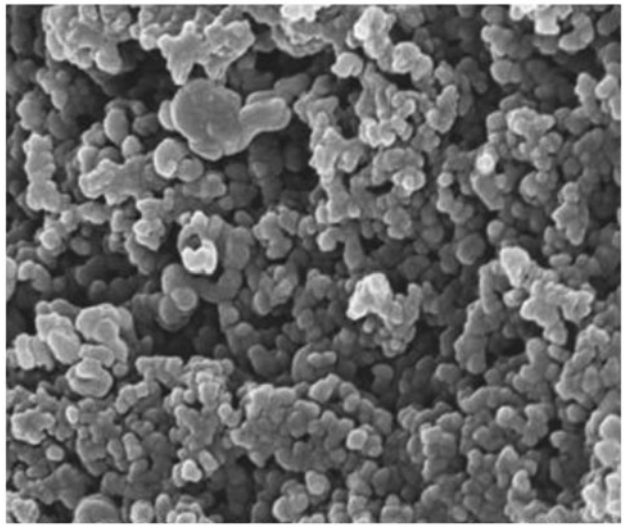

Fig. 1. FESEM image of iron nanocomposite particles.

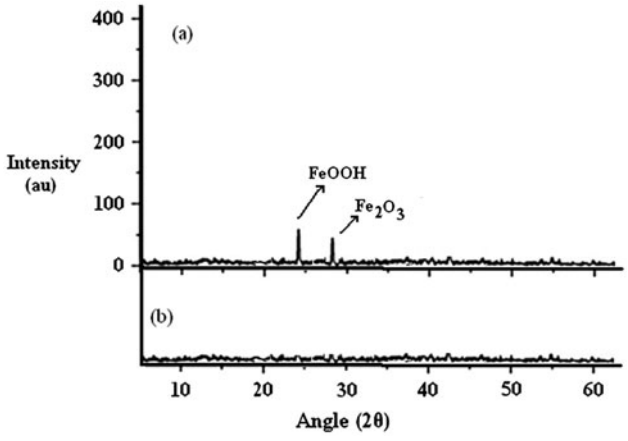

Fig. 2. XRD patterns of (a) native and (b) iron nanocomposited particles.

The calibration curve was linear in the concentration range of 0.10–50 μg/L, with the coefficient of determination (r^2) of 0.999. The LOD was also determined by standard method [24] and found to be 0.4 μg/L.

3.3. Effect of concentration

To optimize the concentration, the experiments were carried out from 5 to 50 μg/L concentration of secbumeton. The other conditions were contact time 30 min., pH 7.0, dose 2.5 g/L, and temperature 20˚C. After adsorption, the adsorbent was filtered and the final concentrations of secbumeton were analyzed. The results are shown in Fig. 3(a), which indicates maximum removal of secbumeton at 30 μg/L. It is clear from this figure that the adsorption increased rapidly from 5 to 30 μg/L concentration. At 5, 10, 20, and 30 μg/L concentrations the adsorption capacities were 2.0, 4.0, 7.80, and 10.8 μg/g. Adsorption became constant after 30 μg/L concentrations even by increasing the concentration up to 50 μg/L. Therefore, it was concluded that 30 μg/L was the optimized concentration. At this concentration the percentage removal was 90 (10.8 μg/g).

3.4. Effect of contact time

The experiments were carried out to determine the effect of contact time (5.0–50.0 min) at 30.0 μg/L concentration of secbumeton at 2.5 g/L dose, 7.0 pH, and 20˚C temperature. The results are given in Fig. 3(b). It is clear from this figure the adsorption capacities were 2.0, 4.0, 6.0, 8.0, 9.5, and 10.8 μg/g at 5, 10, 15, 20, 25, and 30 min contact time, respectively. Further increase in contact time did not result into more adsorption. The percentage removal at 30 min was 90%. It was concluded that the optimum contact time was 30 min.

3.5. Effect of pH

The experiments were also carried out to determine the effect of pH (1.0–10.0) with 30.0 μg/L concentration of secbumeton, 2.5 g/L dose, 30 min contact time and 20.0 temperature ˚C. The results are shown in Fig. 3(c). A perusal of this figure indicates that the adsorption capacities were 2.0, 4.0, 6.0, 7.5, 9.0, 10,8, and 10.8 μg/g at 1.0, 2.0, 3.0, 4.0, 5.0 6.0, and 7.0 pHs, respectively. Further increase in pH could not augment adsorption. The percentage removal at pH 7.0 was 90%. Therefore, this pH was considered as the best one. It was concluded that the method is eco-friendly as most of the water bodies have pH 7.0.

3.6. Effect of dosage

The adsorbent dose was varied from 0.5 to 5.0 g/L with pH 7.0, 30.0 min contact time, 30.0 μg/L concentration of secbumeton at 20˚C temperature. The results of this parameter optimization are given in Fig. 3(d). This figure clearly indicates adsorption capacities 2.0, 5.0, 7.5, 9.5, and 10.8 μg/g at 0.5, 1.0, 1.5, 2.0, and 2.5 g/L adsorbent dose. Further increase in dose did not result in any increase in adsorption. The percentage removal was 90% at 2.5 g/L dose. Therefore, this dose was considered as optimum one. Again, the system was considered economic due to low adsorbent dose. These conditions may be transferred economically at industrial level.

3.7. Effect of temperature

The experiments were carried out to determine the effect of temperature (20.0–30.0˚C) with 30.0 μg/L concentration of secbumeton at pH 7.0, 2.5 g/L dose and 30 min contact time. The results of temperature effects are shown in Fig. 3(e). The uptake of secbumeton was found to decrease with increasing temperature, indicating exothermic nature of the adsorption process. The secbumeton removal followed the order of 20.0 > 25.0 > 30.0˚C. Again the method was considered as eco-friendly as most of water bodies contain temperature from 20 to 30˚C.

3.8. Effect of interfering ions

The present study was carried out with Millipore water. But groundwater contains various ions such as

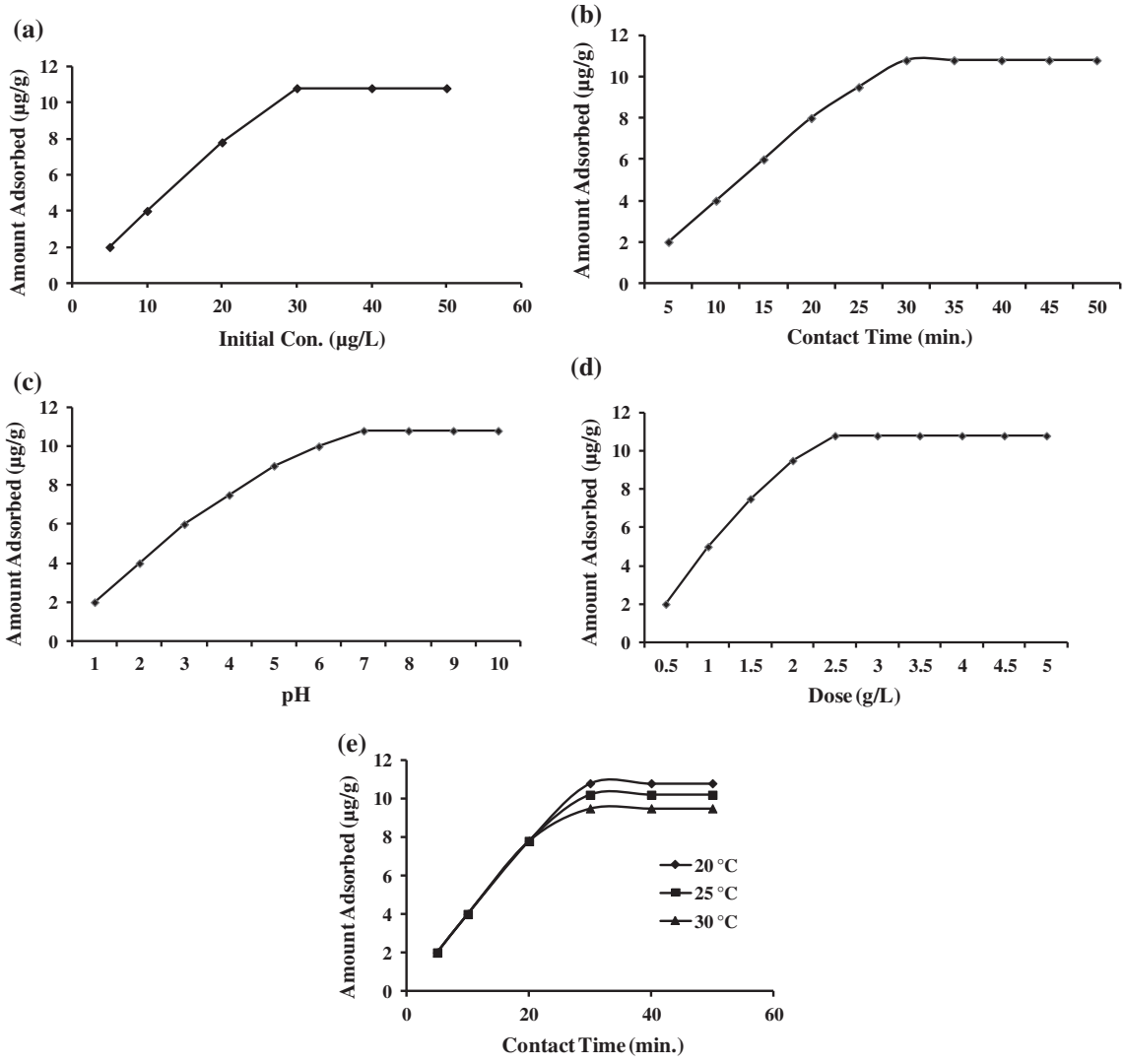

Fig. 3. Optimization of adsorption parameters of secbumeton herbicide; (a) initial conc., (b) contact time, (c) pH, (d) dose, and (e) temperature.

potassium, sodium, magnesium, calcium, sulfate, nitrate, chloride, phosphate, etc. Therefore, the effects of these ions on the adsorption of secbumeton were studied. The experiments were also carried out in the groundwater (laboratory tap water). Groundwater quality of tap water was determined prior to secbumeton adsorption. Conductivity and pH of the ground water were found to be 1.48 mS/cm and 7.19, respectively. The values of total hardness, alkalinity, sodium, potassium, calcium, magnesium, and total dissolved solids (TDS) were 448.0, 280.0, 2.15, 1.84, 204.0, 244.0 mg/L, and 542.25, respectively. It was observed that there was decreased in the adsorption capacity of composite nanomaterial about 0.5–2% for secbumeton (Table 1). The decrease in the adsorption of secbumeton was due to the competitive adsorption between the adsorbate molecules and interfering ions.

3.9. Adsorption isotherms models

The adsorption data was analyzed by using well known models i.e. Langmuir, Freundlich, and Temkin. The experiments for adsorption isotherms were carried out at 20, 30, 35, and 40°C temperatures. The results of these models are discussed in the following sub-sections.

3.9.1. Langmuir adsorption model

Langmuir adsorption isotherm model determines the relationship between the concentrations of surface

Table 1
Effect of interfering ions on the uptake of secbumeton

S. No.	Interfering ions	Maximum percent reduction in the uptake of
1	Sodium	1.0
2	Potassium	1.0
3	Calcium	0.8
4	Magnesium	0.5
5	Chloride	2.5
6	Sulfate	2.0
7	Nitrate	1.8
8	Phosphate	1.2

adsorbed species to the number of active sites on that surface at equilibrium. This model assumes that adsorbate is chemically adsorbed at a fixed number of well defined sites. Once a molecule of adsorbate occupies a site on adsorbent, no further adsorption is possible. Furthermore, all sites are energetically equivalent with no interaction between adsorbate molecules. The applicability of this model indicates monolayer adsorption on a homogeneous surface without interactions between the adsorbed species. Langmuir adsorption isotherm is shown by the following equation.

$$1/Q_e = 1/Q_0 bC_e + 1/Q_0 \quad (3)$$

where C_e and Q_e have usual meaning. Q_0 is the maximum monolayer adsorption capacity of adsorbent (μg/g). b (L/μg) is Langmuir constant related to binding energy of secbumeton onto the active sites of adsorbent. The values of Q_0 provide an estimate of the active sites while b gives an estimate of driving force at equilibrium. The values of Q_0 and b were calculated from slope and intercept of straight line of graph plotted $1/Q_e$ vs. $1/C_e$. Langmuir plots for secbumeton adsorption at 20, 25, and 30˚C are shown in Fig. 4(a). Langmuir model fits the adsorption data of secbumeton onto adsorbent at all the temperatures. The values of regression constants (R^2) were 0.980, 0.992, and 0.997 at 20, 25, and 30˚C, respectively. The values of Langmuir constant (b) were 4.94, 6.40, and 8.67 L/μg at 20, 25, and 30˚C (Table 2), indicating good binding of secbumeton at all the temperatures. The values of Q_0 were 11.24, 10.42, and 9.62 μg/g at these temperatures. The values of dimensionless constant [separation factor (R_L)] were calculated by the following equation.

$$R_L = 1/(1 + bC_e) \quad (4)$$

These values were 0.067, 0.035, and 0.019 at 20, 25, and 30˚C, respectively. The values of R_L lower than 1.0 indicates energetically favorable adsorption. Furthermore, it was concluded that R_L value was the lowest at 20˚C; indicating more favorable adsorption at low temperature.

3.9.2. Freundlich isotherm

Freundlich isotherm is the most important multisite adsorption isotherm for rough surfaces. Freundlich isotherm adsorption does not restrict to monolayer only, but multilayer adsorption with non uniform distribution of adsorption heat and affinities over the heterogeneous surface. The amount of adsorbate adsorbed on the surface of adsorbent is the summation of all sites. The adsorption energies decrease exponentially on the completion of adsorption process. Freundlich adsorption isotherm is given by the following equation.

$$\log Q_e = (1/n) \log C_e + \log K_F \quad (5)$$

where K_F [(μg/g)] and n are empirical constants called Freundlich constants; K_F corresponds to the relative adsorption capacities of the adsorbent and n is the adsorption intensity. The values of n from 1 to 10 are indication of favorable adsorption. The plot of log Q_e vs. log C_e is straight line and the intercept corresponds to K_F. The slope ($1/n$) is a measure of adsorption intensity. Freundlich isotherm plots for secbumeton adsorption are shown in Fig. 4(b) with constants values in Table 2. The values of K_F were 6.73, 6.40, and 6.07 at 20, 25, and 30˚C, respectively. The values of n were 4.49, 4.77, and 5.16, indicating favorable adsorption. The regression coefficients at all three temperatures were close to unity, confirming the best fitting of Freundlich model.

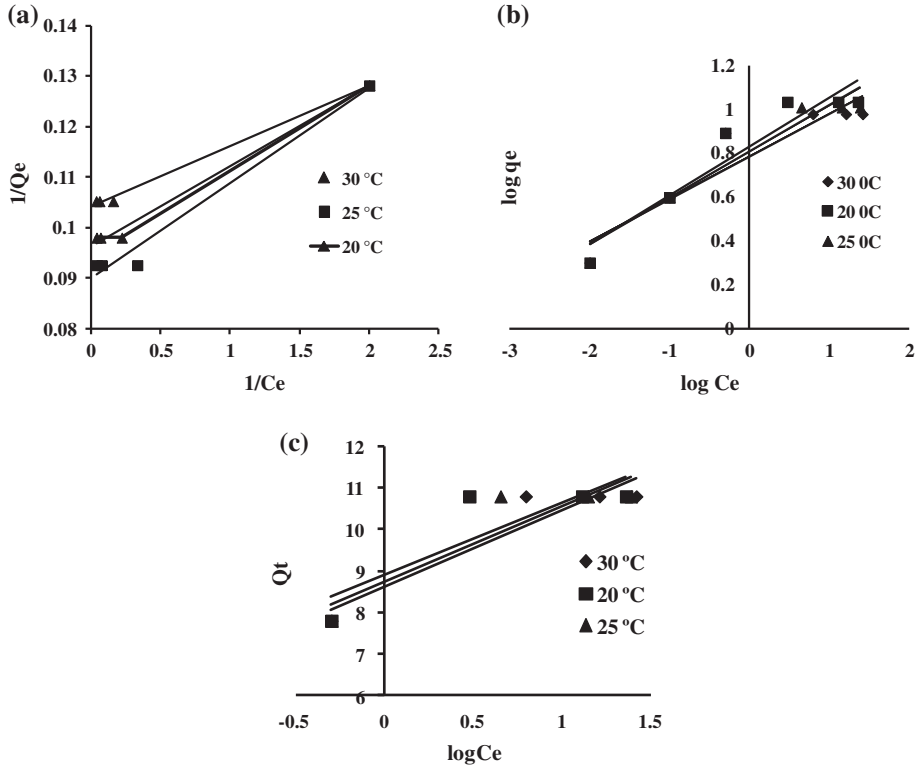

Fig. 4. The plots showing (a) Langmuir, (b) Freundlich, and (c) Temkin isotherms for the removal of secbumeton herbicide.

Table 2
Isotherm parameters values for secbumeton

	Langmuir isotherm				Freundlich isotherm			Temkin isotherm		
Temp. (℃)	Q_0 (μg/g)	b (L/μg)	R_L	R^2	K_F (μg/g)	n (g/L)	R^2	K_T (L/g)	B_T (kJ/mol)	R^2
20	11.24	4.94	0.067	0.980	6.73	4.49	0.901	162.42	1.39	0.748
25	10.42	6.40	0.035	0.992	6.40	4.77	0.898	117.69	1.35	0.831
30	9.62	8.67	0.019	0.997	6.07	5.16	0.880	107.31	1.33	0.884

3.9.3. Temkin isotherm

The adsorbate interactions with adsorbent are described by Temkin model. It isotherm assumes that heat of adsorption of all the molecules in the layer decreases linearly with increasing surface coverage due to adsorbate–adsorbate interactions. Furthermore, adsorption is characterized by a uniform distribution of binding energies; up to some maximum binding energy. Temkin isotherm is given by the following equation.

$$Q_e = (RT/B_T) \ln C_e + (RT/B_T) \ln K_T \quad (6)$$

where K_T (L/g) is the equilibrium binding constant showing maximum binding energy. B_T constant is related to the heat of adsorption. R is the ideal gas constant (0.008314 kJ/mol/K). T is the temperature in Kelvin. A plot of Q_t vs. log C_e for secbumeton was linear (Fig. 4(c)). The isotherm constants B_T and K_T were calculated from the slope and the intercept, respectively (Table 2). The values of K_T were 162.42, 117.69, and 107.31 L/g at 20, 25, and 30℃, respectively, indicating strong interactions between adsorbate and adsorbent. The values of B_T were 1.39, 1.35, and 1.33, indicating small variation in the heat of adsorption. The values of regression coefficient (R^2) were close to

unity showing the applicability of Temkin isotherm to the experimental data.

3.10. Thermodynamic study

The thermodynamic process was determined by calculating free energy, enthalpy, and entropy. Gibbs free energy change of the adsorption is related to the equilibrium constant by Vant Hoffs equation.

$$\Delta G^0 = -RT \ln K \quad (7)$$

where ΔG°, T, R, and K are free energy change (kJ/mol), absolute temperature (K), universal gas constant (0.008314 kJ mol^{-1} K^{-1}), and equilibrium constant, respectively. By replacing K by Q^o (Langmuir constant), the equation changes to the following form.

$$\Delta G^0 = -RT \ln Q^o \quad (8)$$

The values of ΔG° at 20, 25, and 30°C were calculated and found −5.89, −5.81, and -5.71 kJ mol^{-1} (Table 3). The negative values of ΔG° confirmed the adsorption process to be favorable and spontaneous. Gibbs free energy of adsorption (ΔG°) is related with changes in entropy (ΔS°) and enthalpy (ΔH°) by the following equations.

$$\Delta G^0 = \Delta H^0 - T\Delta S^0 \quad (9)$$

The above equation can be changed to the following form.

$$\ln(Q^o) = \Delta S^0/R - \Delta H^0/RT \quad (10)$$

A plot of ln Q^ovs. $1/T$ was a straight line (graph not shown). The intercept gave the value of ΔS° while slope belongs to ΔH°. The values of ΔH° and ΔS° were −11.08 and -1.78×10^{-2}, respectively. The negative value of enthalpy change indicated exothermic adsorption. The low negative value of ΔS° showed decreased entropy of adsorption process. Therefore, it was assumed that adsorption of secbumeton was associated with decline in mobility freedom of secbumeton.

3.11. Kinetic modeling

Adsorption mechanism may be determined by kinetic modeling, which depends on the physical and chemical features of the adsorbate and adsorbent. In view of these facts, different models were tested using adsorption data. These are discussed in the following sub-sections.

3.11.1. Pseudo-first-order kinetic model

This is the first model used for mechanism determination. It is given by the following equation.

$$dQ_t/dt = K_1(Q_e - Q_t) \quad (11)$$

The above equation was integrated with boundary conditions, $t = 0$ with $Q_t = 0$ and $t = t$ with $Q_t = Q_t$, to obtain lineralized equation as given below.

$$\log (Q_e - Q_t) = \log Q_e - k_1 t/2.303 \quad (12)$$

where Q_e, Q_t, and k_1 (min^{-1}) are solute amount (μg/g) adsorbed at equilibrium, at time any time and equilibrium rate constant of pseudo-first-order sorption. All these values are given in Table 4. The rate constant was calculated by plotting log ($Q_e - Q_t$) vs. t (Fig. 5(a)) at 20°C temperature. The pseudo-first-order rate constant was 0.094 (min^{-1}) with 0.9577 as regression coefficient (R^2); indicating fitness of pseudo-first-order model. The experimental and theoretical values of Q_e were 10.8 and 16.51 μg/g, respectively, with 52.87% higher theoretical value. Hence, pseudo-first-order kinetic model did not fit best to the experimental data. This sort of discrepancies have also been reported by other workers [25–27]. In view of these facts, the attempts have been made to shift to pseudo-second-order kinetic model.

Table 3
Thermodynamic parameter values for secbumeton

ΔG° (kJ/mol)				
T = 293 K	T = 298 K	T = 303 K	ΔH° (kJ/mol)	ΔS° (kJ/mol K)
−5.89	−5.81	−5.71	−11.08	-1.78×10^{-2}

Table 4
Kinetic parameters for secbumeton adsorption

Kinetic model	Kinetic parameters	Numerical value
Pseudo-first-order kinetic model	k_1 (min^{-1})	0.094
	Experimental Q_e (μg/g)	10.8
	Theoretical Q_e (μg/g)	16.51
	R^2	0.9577
Pseudo-second-order kinetic model	k_2 (g μg^{-1} min^{-1})	7.1×10^{-3}
	Experimental Q_e (μg/g)	10.8
	Theoretical Q_e (μg/g)	13.47
	h (μg g^{-1} min^{-1})	1.28
	R^2	0.9625
Elovich kinetic model	α (μg g^{-1} min^{-1})	14.44
	β (g μg^{-1})	0.23
	R^2	0.9518
Intraparticle diffusion kinetic model	k_{ipd1} (μg g^{-1} $min^{-0.5}$)	5.78
	Intercept	4.51
	R^2	0.9954
Film diffusion kinetic model	k_{fd} (g μg^{-1})	0.094
	Intercept	0.43
	R^2	0.954

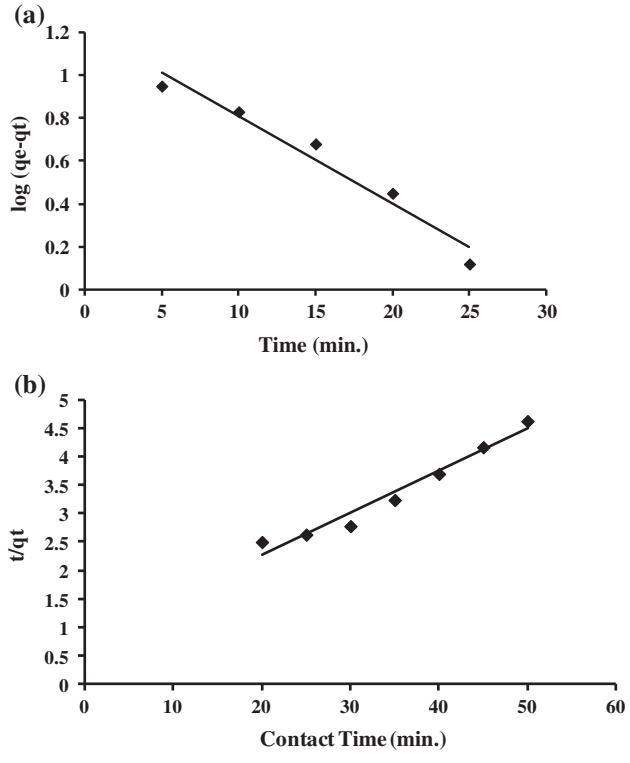

Fig. 5. The plots showing (a) pseudo-first-order kinetic plot and (b) pseudo-second-order kinetic plot.

3.11.2. Pseudo-second-order kinetic model

Pseudo-second-order kinetic model is based on chemical or exchange type of adsorption. Pseudo-second-order kinetic model for adsorption phenomenon is given by the following equation.

$$dQ_t/dt = K_2(Q_e - Q_t)^2 \quad (13)$$

where Q_e, Q_t, and t have the same meanings as explained above. The above equation was integrated with boundary conditions, $t = 0$ with $Q_t = 0$ and $t = t$ with $Q_t = Q_t$; resulting into the following equation.

$$t/Q_t = 1/k_2Q_e^2 + t/Q_t \quad (14)$$

In the above equation $k_2Q_e^2$ was replaced by h, resulting into the following equation.

$$t/Q_t = 1/h + t/Q_e \quad (15)$$

where h is initial adsorption rate constant. It was obtained from pseudo-second-order plot. Q_t/t became h as time approached to zero. k_2 is rate constant of pseudo-second-order adsorption (g/μg/min). A graph between t/Q_t vs. t was plotted (Fig. 5(b)). Q_e and k_2 were calculated from slope and intercept of the plot. The calculated parameters are given in Table 4. k_2 value of adsorption was 7.1×10^{-3} g μg^{-1} min^{-1}; very small as compared to initial rate constant ($h = 1.28$ g μg^{-1} min^{-1}). These data confirmed fast speed of adsorption initially followed by slow speed with increase of time. The regression coefficient ($R^2 = 0.9625$) was high showing the applicability of

pseudo-second-order model of adsorption process. Moreover, theoretical and experimental Q_e values were in good agreement as compared to in pseudo-first-order kinetic model. Therefore, the applicability of pseudo-first-order kinetic model was confirmed.

3.11.3. Elovich's kinetic model

Elovich's kinetic model is used to predict rate of adsorption and desorption phenomenon. Originally, Elovich equation was developed to describe the kinetics for chemo-adsorption of gases to the solid surfaces. Later on, it was modified by Chien and Clayton [28] assuming increase in activation energy of adsorption linearly with surface coverage. This model is given by the following equation.

$$dQ_t/dt = \alpha \exp(-\beta Q_t) \quad (16)$$

where α (μg/g/min) indicates initial adsorption rate. β desorption constant (g/μg) shows rate during any experimental time. The above equation was integrated using the boundary conditions, $t = 0$ with $Q_t = 0$ and $t = t$ with $Q_t = Q_t$. Further assuming $\alpha\beta t >> 1$, Eq. (16) becomes in the following form.

$$Q_t = 1/\beta \cdot \ln(\alpha\beta) + 1/\beta \ln t \quad (17)$$

The experimental data was fitted to this model. The values of α, β, and R^2 are given in Table 4. The values of α, β and R^2 were 14.44 μg g^{-1} min^{-1}, 0.23 g μg^{-1}, and 0.9518, respectively, suggesting higher rate of adsorption than desorption. The values of α and β confirmed fast adsorption initially, followed by a decrease in adsorption process with increase of time. Moreover, value of regression constant was close to unity, indicating the applicability of this model.

3.12. Adsorption mechanism

Generally, adsorption process is occurred via film diffusion, pore diffusion, and intra-particle diffusion mechanism. The slowest step is rate determining one, controlling adsorption process. The data were tested with intraparticle and film diffusion models to evaluate the mechanism of uptake of secbumeton on composite nanomaterial.

3.12.1. Intraparticle diffusion kinetic model

The adsorption of adsorbate on adsorbent surface comprises different processes i.e. (i) transport of adsorbate from bulk solution by liquid film to adsorbent surface, (ii) adsorption of adsorbate on adsorbent surface, and (iii) transport of adsorbate within the pores of adsorbent. Therefore, adsorption mechanism is controlled either by surface adsorption kinetics or transport phenomenon (film and intraparticle diffusions) mechanism or by both processes. The second step is very rapid and cannot be rate determining. First and third steps may be rate-determining ones. Therefore, these steps were studied by two models. The transport of secbumeton from solution to adsorption sites may be studied by relationship between amount of adsorbed secbumeton and square root of contact time. The equation for this is given below.

$$Q_t = k_{ipd} t^{0.5} \quad (18)$$

If a graph plotted Q_t vs. $t^{0.5}$ is a straight line passing through the origin, and slope of the line corresponds to rate constant (k_{ipd}), the adsorption is controlled by intra-particle diffusion. This graph was drawn (figure not given) and the value of rate constant 5.78 μg g^{-1} $min^{-0.5}$. The values of intercept and regression coefficient were 4.51 and 0.9954, respectively (Table 4). The graph line did not pass through the origin indicating that adsorption did not control by intra-particle diffusion.

3.12.2. Liquid film diffusion kinetic model

Liquid film diffusion kinetics model was given by Boyd et al. [29]. In this model, boundary plays a significant role in the adsorption process. Liquid film diffusion model is given by the following equation.

$$\ln(1 - Q_t/Q_e) = -k_{fd} t \quad (19)$$

Or

$$\ln(1 - F) = -k_{fd} t \quad (20)$$

where F (Q_t/Q_e) is the fractional attainment of equilibrium. k_{fd} is film diffusion rate constant. If a graph of ln $(1 - F)$ vs. t is a straight line with zero intercept, the adsorption is supposed to proceed via film diffusion mechanism. The values of film diffusion rate constant, intercept, and regression constant (R^2) were 0.094 g μg^{-1}, 0.43, and 0.954, respectively (Table 4). The straight line passed through origin with small deviation from zero intercept (−0.4258). This deviation from zero might be due to high speed of agitation used during the kinetic experiments. Moreover, the difference

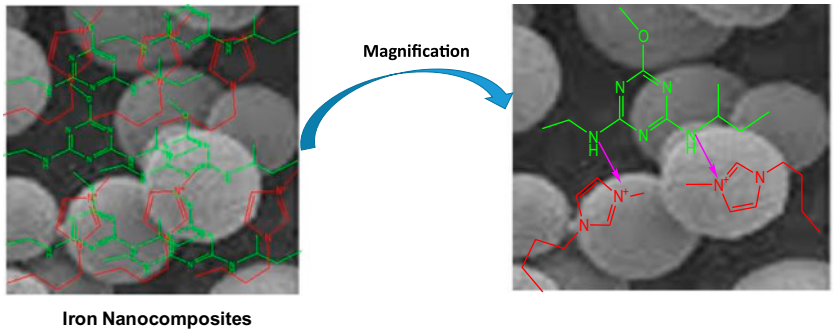

Fig. 6. Mechanism of secbumeton herbicide adsorption.

between rate of mass transfer in the initial and final steps of adsorption process might be responsible for small deviation from zero. The similar results are also available into the literature [30–32]. Therefore, adsorption of secbumeton on nanocomposite adsorbent is controlled by liquid film diffusion mechanism.

4. Mechanism of adsorption at supra-molecular level

It is assumed that NPs are good adsorbents for the removal of different pollutants. Moreover, the reported nano iron composite material has positive charge. Therefore, it has good attractive tendencies to hold secbumeton herbicide on the surface. The schematic representation of secbumeton herbicide removal by adsorption is shown in Fig. 6. It is clear from this figure that nano iron composite material has positive charges; giving opportunities to nitrogen lone pairs of secbumeton herbicide to co-ordinate. Therefore, secbumeton herbicide molecules form co-ordination bonding with nanocomposite material.

Therefore, the removal of secbumeton herbicide on the reported adsorbent is controlled by chemical bonding. That is why the reported method is fast for the removal of fluoride from water.

5. Desorption studies

For an economical process, the adsorbent should be regenerable and recyclable. Therefore, attempts have been made to regenerate the adsorbent and recycling. The regeneration was carried out by hydrochloric acid, nitric, and sulfuric acids. The best regeneration reagent was achieved using hydrochloric acid. It was observed that maximum desorption (99%) was obtained with HCl (0.01 N). The regenerated adsorbent was used for consecutive seven cycles for the removal of secbumeton. The removal capacities for seven cycles ranged from 90 to 98%.

6. Application of the developed method in real water samples

The applicability of any method is determined by the fact if it is applicable to solve real world problem. Therefore, the developed adsorption method was applied to remove secbumeton herbicide from river water samples. Ten water samples were collected from different location in the river Yamuna, New Delhi, India. The concentrations of this herbicide in collected water samples ranged from 1.0 to 20 μg/L. The reported adsorption method was applied to remove secbumeton herbicide from river water samples. The procedure was as described into the experimental section. It was observed that the percentage removal of secbumeton herbicide ranged from 90 to 100%. This section of the paper evidently showed that the developed adsorption method was applicable for the removal of secbumeton herbicide from natural river water.

7. Conclusion

It is clear from the results that the developed nanocomposite material (adsorbent) is capable to remove secbumeton organic pollutant from water successfully. The adsorption method was selective for secbumeton. The percentage removal of secbumeton from water was 90%. The adsorption process was exothermic with $20 > 25 > 30$°C as the order of removal capacities. GC–MS method was capable to detect trace level of secbumeton with 0.4 μg/L as detection limit. The adsorption followed Langmuir, Freundlich, and Temkin models. Thermodynamic studies indicated that adsorption is exothermic in nature. Kinetic modeling showed pseudo-second-order and liquid film diffusion mechanisms. Briefly, the developed adsorption method is fast, eco-friendly, and economic as may be used at pHs of natural water bodes with low contact time and dose. Low contact

time is the best feature of this method making the results transferable at column operation. Therefore, reported method may be used for the removal of secbumeton from any water body at large scale economically.

Acknowledgment

The authors are thankful to King Saud University, Riyadh, Saudi Arabia for Visiting Professor Program.

References

[1] I. Ali, H.Y. Aboul-enein, Leaching of triazine pesticides in loamy soil and their determination by reversed phase HPLC, Int. J. Environ. Anal. Chem. 81 (2001) 315–322.
[2] V.K. Gupta, I. Ali, Analysis of atrazine and its degradation products in loamy soil by SPE and HPLC, Int. J. Environ. Pollut. 27 (2006) 204–210.
[3] H.H. See, M.M. Marsin Sanagi, W.A. Ibrahim, Determination of triazine herbicides using membrane-protected carbon nanotubes solid phase membrane tip extraction prior to micro-liquid chromatography, J. Chromatogr. A 1217 (2010) 1767–1772.
[4] J.T. Stevens, D.D. Sumner, Herbicides, in: W.J. Hayes Jr., E.R. Laws Jr. (Eds.), Handbook of Pesticide Toxicology, Academic Press, New York, NY, 1991, pp. 1341–1343.
[5] National Library of Medicine, Hazardous Substances Databank 8 (1995) 17–34.
[6] J.A. Van Leeuwen, D. Waltner-Toews, T. Abernathy, B. Smit, M. Shoukri, Associations between stomach cancer incidence and drinking water contamination with atrazine and nitrate in Ontario (Canada) agroecosystems, 1987–1991, Int. J. Epidemiol. 28 (1999) 836–840.
[7] B. De Ventura Campo, D. de Angelis Fransceschi, M.A. Marin-Morales, Mutagenic and genotoxic effects of the atrazine herbicide in *Oreochromis niloticus* (Perciformes, Cichlidae) detected by the micronuclei test and the comet assay, Biochem. Physiol. 90 (2008) 42–51.
[8] C. Nakamura, M. Hasegawa, K. Shimada, M. Shirai, J. Miyake, Direct triazine herbicide detection using a self-assembled photosynthetic reaction center from purple bacterium, Biotech. Bioprocess Eng. 5 (2000) 413–417.
[9] M.M. Sanagi, SS. Muhammad, I. Hussain, W.A.W. Ibrahim, I. Ali, Novel solid-phase membrane tip extraction and gas chromatography with mass spectrometry methods for the rapid analysis of triazine herbicides in real waters, J. Sep. Sci. 38 (2015) 433–438.
[10] US EPA, The Determination of Triazine Pesticides in Municipal and Industrial Wastewater, Method 619. Available from: <http://www.accustandard.com/assets/619.pdf>.
[11] A. Alvarsson, Assessing the Environmental Impact of Pesticides; Effects of Photosystem II Inhibiting Herbicides on Primary Production and Ecosystems, Degree Project for Master of Science in Ecotoxicology 30 ECTS, Department of Biology and Environmental Sciences, University of Gothenburg, Sweden, 2012.
[12] I. Ali, V.K. Gupta, Advances in Water Treatment by Adsorption Technology, Nature London 1 (2006) 2661–2667.
[13] I. Ali, The quest for active carbon adsorbent substitutes: Inexpensive adsorbents for toxic metal ions removal from wastewater, Sep. Purif. Rev. 39 (2010) 95–171.
[14] I. Ali, M. Asim, T.A. Khan, Low cost adsorbents for the removal of organic pollutants from wastewater, J. Environ. Manage. 113 (2012) 170–183.
[15] I. Ali, Water treatment by adsorption columns: Evaluation at ground level, Sep. Purif. Rev. 43 (2014) 175–2015.
[16] M.L. Yola, T. Eren, N. Atar, A novel efficient photocatalyst based on TiO_2 nanoparticles involved boron enrichment waste for photocatalytic degradation of atrazine, Chem. Eng. J. 250 (2014) 288–294.
[17] N. Atar, A. Olgun, S. Wang, Adsorption of cadmium (II) and zinc (II) on boron enrichment process waste in aqueous solutions: Batch and fixed-bed system studies, Chem. Eng. J. 192 (2012) 1–7.
[18] N. Atar, A. Olgun, Removal of basic and acid dyes from aqueous solutions by a waste containing boron impurity, Desalination 249 (2009) 109–115.
[19] N. Atar, A. Olgun, S. Wang, S. Liu, Adsorption of anionic dyes on boron industry waste in single and binary solutions using batch and fixed-bed systems, J. Chem. Eng. Data 56 (2011) 508–516.
[20] I. Ali, New generation adsorbents for water treatment, Chem. Rev. 112 (2012) 5073–5091.
[21] L. Huang, X. Weng, Z. Chen, M.M.R. Naidu, Green synthesis of iron nanoparticles by various tea extracts: Comparative study of the reactivity. Spectrochim, Spectrochim. Acta, Part A 130 (2014) 295–301.
[22] T. Shahwan, S. Abu Sirriah, M. Nairat, E. Boyacı, A.E. Eroğlu, T.B. Scott, K.R. Hallam, Green synthesis of iron nanoparticles and their application as a Fenton-like catalyst for the degradation of aqueous cationic and anionic dyes, Chem. Eng. J. 172 (2011) 258–266.
[23] G.E. Hoag, J.B. Collins, J.L. Holcomb, J.R. Hoag, M.N. Nadagouda, R.S. Varma, Degradation of bromothymol blue by 'greener' nano-scale zero-valent iron synthesized using tea polyphenols, J. Mater. Chem. 19 (2009) 8671–8677.
[24] D.G. Watson, Pharmaceutical Analysis: A Text Book of Pharmacy Students and Pharmaceutical Chemists, John Wiley & Sons, London, 1999.
[25] T.A. Khan, S.A. Chaudhry, I. Ali, Equilibrium uptake, isotherm and kinetic studies of Cd(II) adsorption onto iron oxide activated red mud from aqueous solution, J. Mol. Liq. 202 (2015) 165–175.
[26] Y.S. Ho, G. Mckay, The kinetics of sorption of basic dyes from aqueous solution by sphagnum moss peat, Can. J. Chem. Eng. 76 (1998) 822–827.
[27] K.G. Bhattacharyya, A. Sharma, Kinetics and thermodynamics of methylene blue adsorption on Neem leaf powder, Dyes Pigm. 65 (2005) 51–59.
[28] S.H. Chien, W.R. Clayton, Application of Elovich equation to the kinetics of phosphate release and sorption in soils1, Soil Sci. Soc. Am. J. 44 (1980) 265–268.

[29] G.E. Boyd, A.W. Adamson, L.S. Myers, The exchange adsorption of ions from aqueous solutions by organic zeolites. II. Kinetics 1, J. Am. Chem. Soc. 69 (1947) 2836–2848.
[30] C.W. Cheung, J.F. Porter, G. Mckay, Sorption kinetic analysis for the removal of cadmium ions from effluents using bone char, Water Res. 35 (2001) 605–612.
[31] M. Onyango, H. Matsuda, T. Ogada, Sorption kinetics of arsenic onto iron-conditioned zeolite, J. Chem. Eng. Jpn. 36 (2003) 477–485.
[32] S. Goswami, U.C. Ghosh, Studies on adsorption behaviour of Cr(VI) onto synthetic hydrous stannic oxide, Water SA 31 (2005) 57–602.